Vertical Propagation of Near-Inertial Waves in a complex Vorticty Field

Daniel Rudloff, Johannes Karstensen, Tim Fischer, Florian Schütte, Arne Bendinger, Sabrina Speich, Pierre L'Hegaret, Xavier Carton, Gilles Reverdin, Rémi Laxenaire, and Jonathan Gula

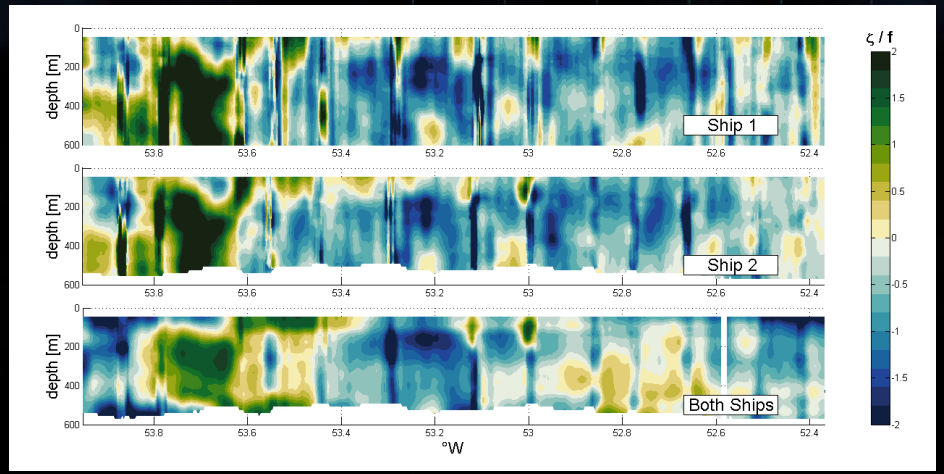

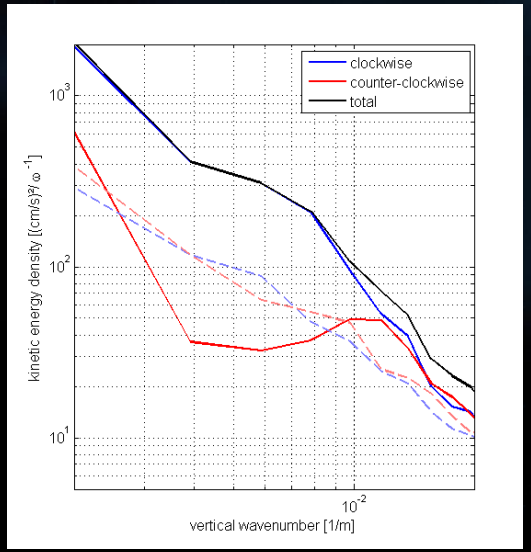

Two Ship Section

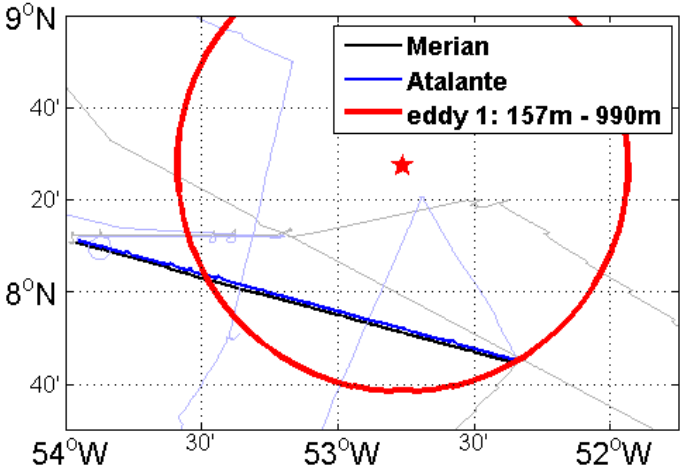

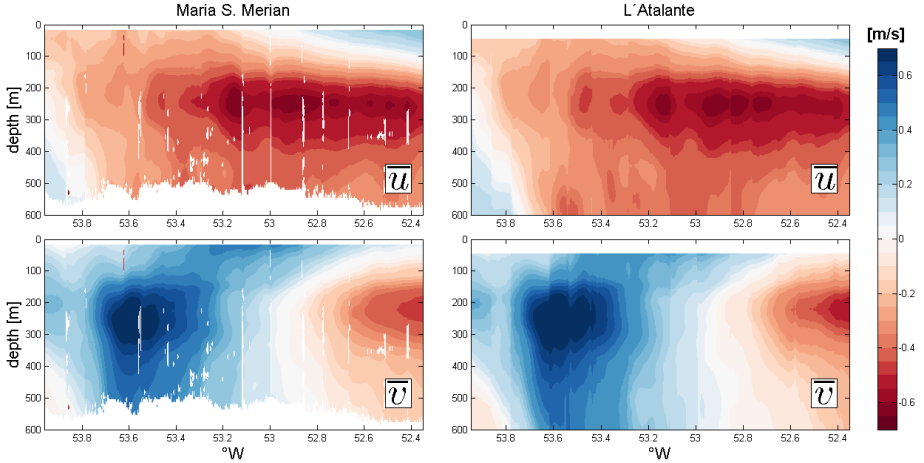

- 180km long section where both ships operated approximately 1.8km apart
- Majority of the section inside deep reaching subsurface anticyclone
- Filtered (180m x 8km) velocities (upper right) used for vorticity calculation

Vorticity calculation

One ship solution:

- Coordinate system is rotated to create 45° angle between ship track and either axis
- u and v data points are projected onto new x- and y- axis
- Linear regression along rotated x or y axis of u or v to get $\frac{\partial u}{\partial x}$, $\frac{\partial u}{\partial y}$, $\frac{\partial v}{\partial x}$ and $\frac{\partial v}{\partial y}$

Calculation of $\frac{\partial u}{\partial y}$ and $\frac{\partial v}{\partial y}$:

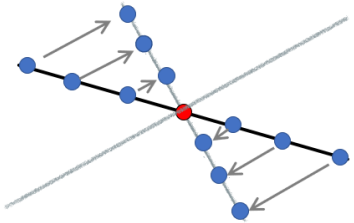

Calculation of $\frac{\partial u}{\partial x}$ and $\frac{\partial v}{\partial x}$:

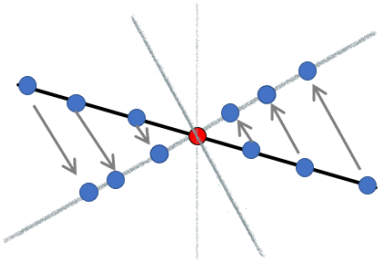

Two ship solution:

(Shcherbina et al., 2013)

$$\zeta = \frac{dv}{dx} - \frac{du}{dy}$$

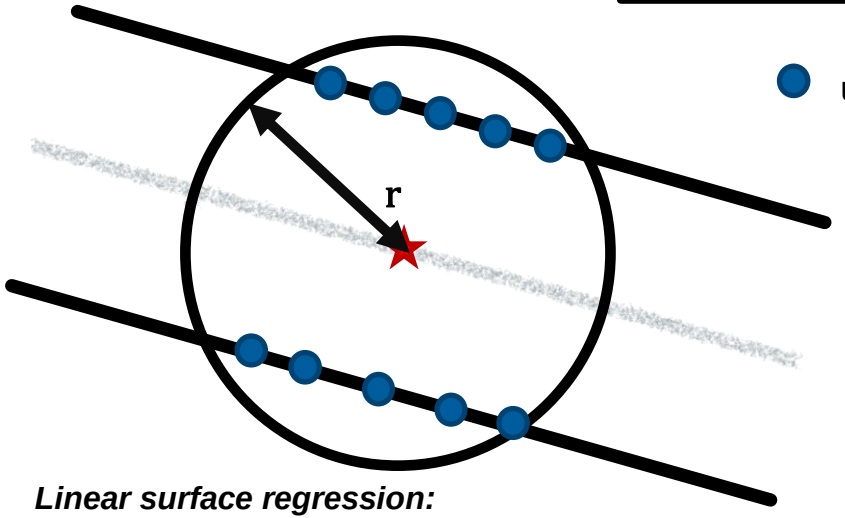

Linear surface regression:

$$u(x,y) = u_0 + u_x * x + u_y * y$$
$$v(x,y) = v_0 + v_x * x + v_y * y$$

Vorticity Comparison

One-ship solution using only data of RV L'Atalante

One-ship solution using only data of RV Maria S Merian

Two-ship Solution using data from both vessels

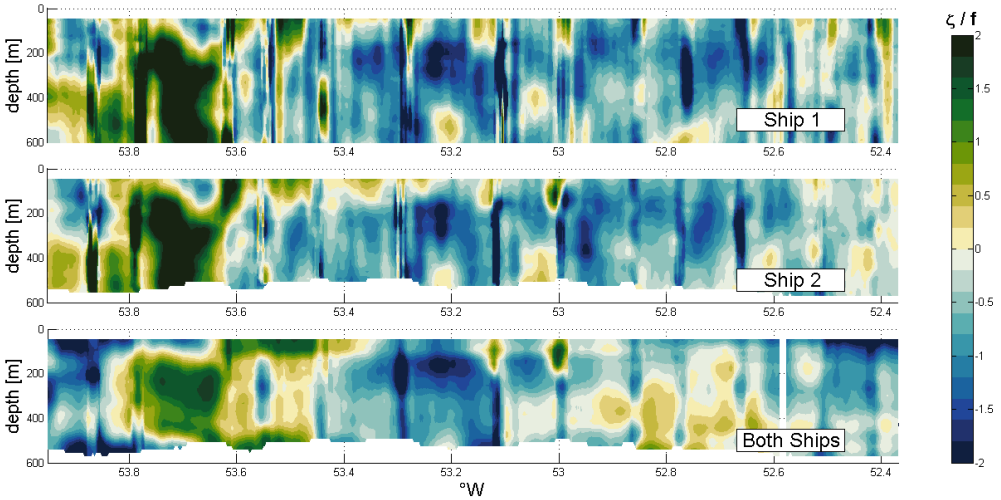

Comparison:

Over all structures fits well

Structure of positive Vorticity around 53.7°W strongly overestimated by both on-ship solution

Positive structure below 200m at 52.5°W – 52.9°W not captured in one-ship solution at all

Vorticity Comparison

Precision of 1-Ship Solutions:

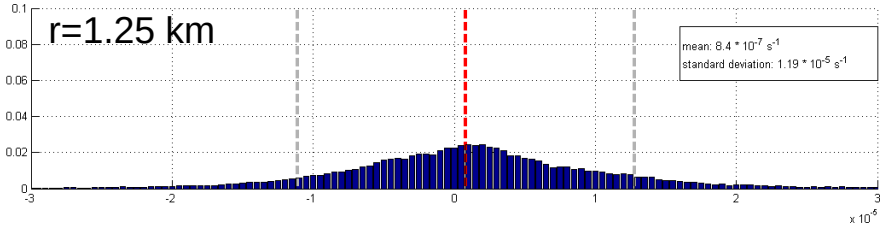

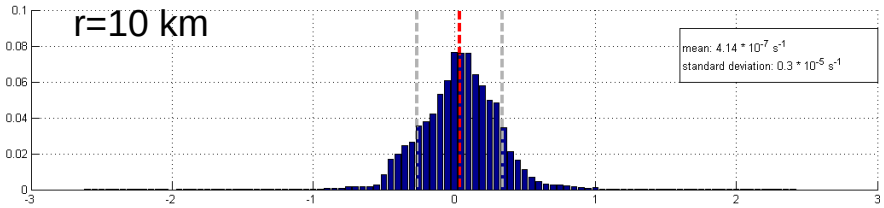

Accuracy is drastically increased by taking larger influence radii

Uncertainty is comparable to Rudnick et al., 2001

→ r = 10 km is used in this study

Accuracy of 1-Ship Solutions:

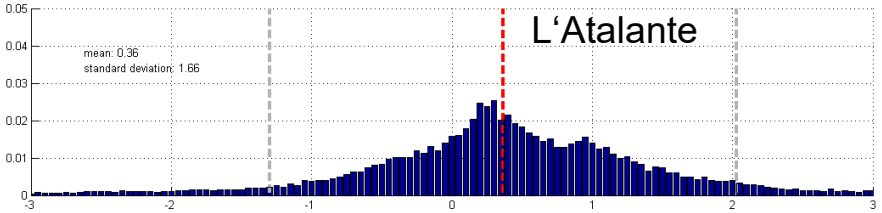

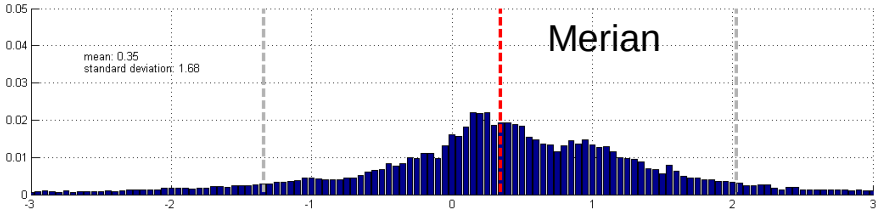

Overestimation of 35% of the vorticity

Uncertainty of the error dominating

Analysis of observed velocity sections

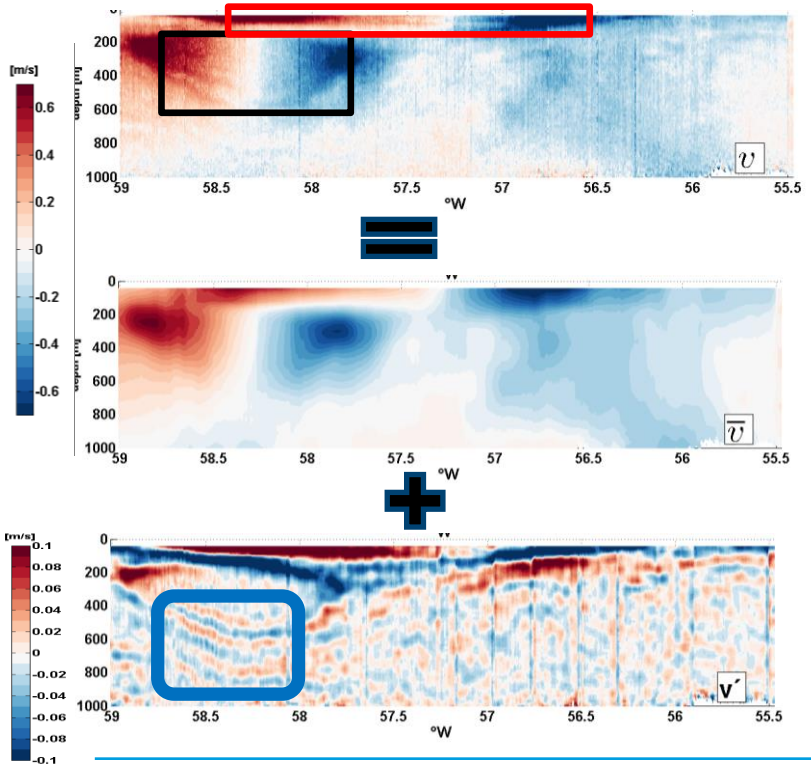

Observed velocities are split up:

$$u = \bar{u} + u'$$

,where $\bar{u}$ derived by applying linear boxcar filter (180m x 8km) to the observed velocity field.

$\bar{u}$ is used to derive eddies. Rankine Vortices are fitted to the velocity field using a Gauss-Newton Optimization (Castelão & Johns, 2011)

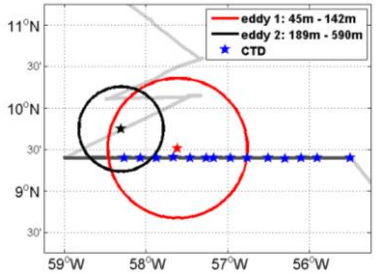

u' is used for detection and characterisation of near-inertial Waves. Wave length calculated via phase angle. Phase velocity via Radon Transform (Challenor, 2001).

Mesoscale Eddy field

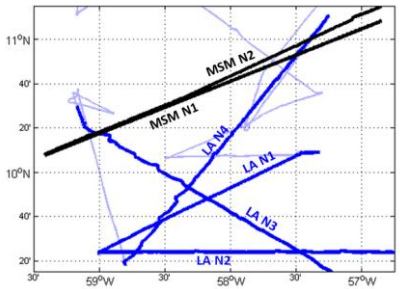

The same eddy structure was crossed at six different times. For each crossing a surface (solid line) and a subsurface (dashed line) anticyclone could be derived.

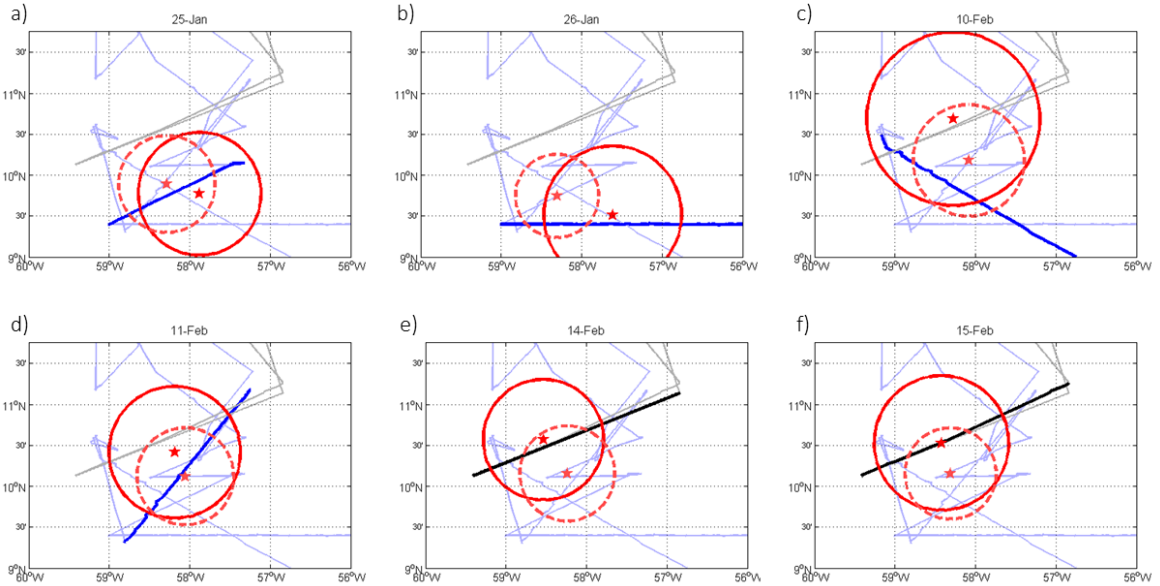

The section on which the derivation of the eddies is based is highlighted in each subplot. Note the translation of both eddies between 25th,26th January (a) and b)) and 10th to 15th February (c) – f))

Observed Near Inertial Waves

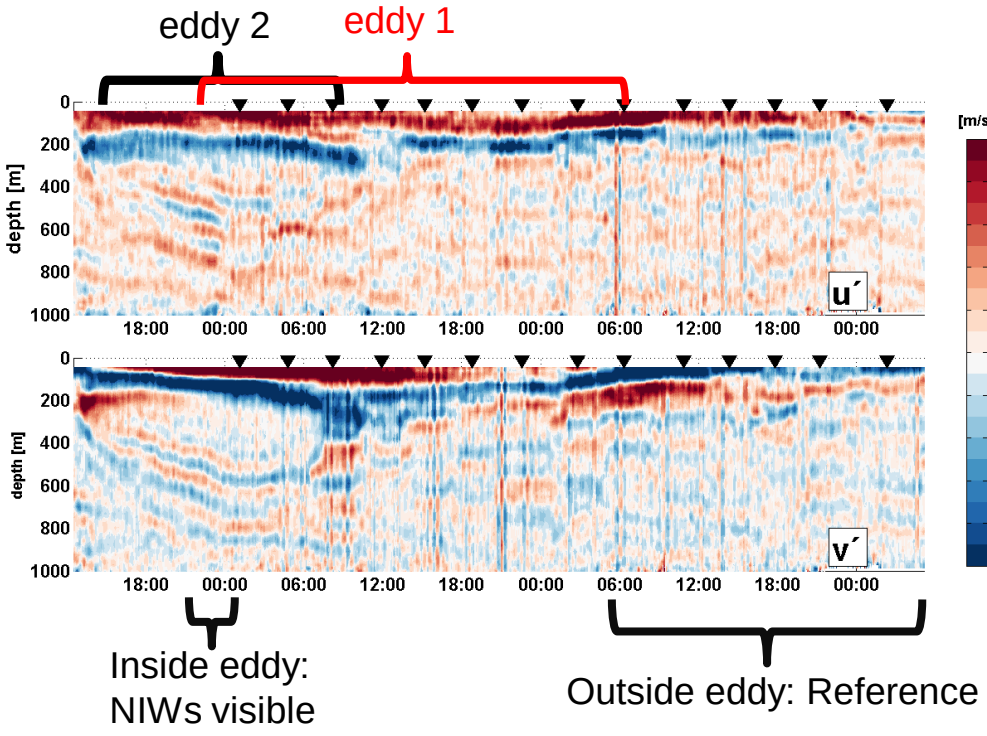

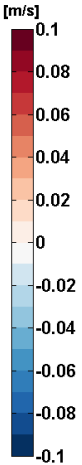

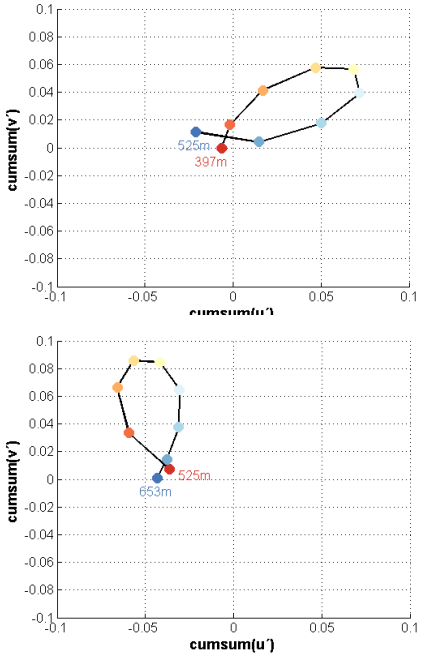

Progressive Vector Diagrams:
Averaged over 90 profiles at a location inside the eddy where NIWs are visible.
Upper: 420m – 520m
Lower: 520m – 650m

Both diagrams show clockwise rotation of the velocity vector with increasing depth with a wave length of about 130m

Observed Near Inertial Waves

Methodology of rotated power spectra described in Mooers, 1973 and Leaman and Sanford, 1975.

Faded lines based on velocity profiles from region indicated as ‘Outside Eddy: Reference’ on previous slide. Solid lines from time span indicated as ‘inside Eddy: NIWs visible’.

NIWs inside the eddy are linked to the downward energy propagation for vertical wavelength between 100m and 300m.

Also, the total amount of kinetic energy is higher inside an eddy.
These results are supported by the analysis of different eddies.

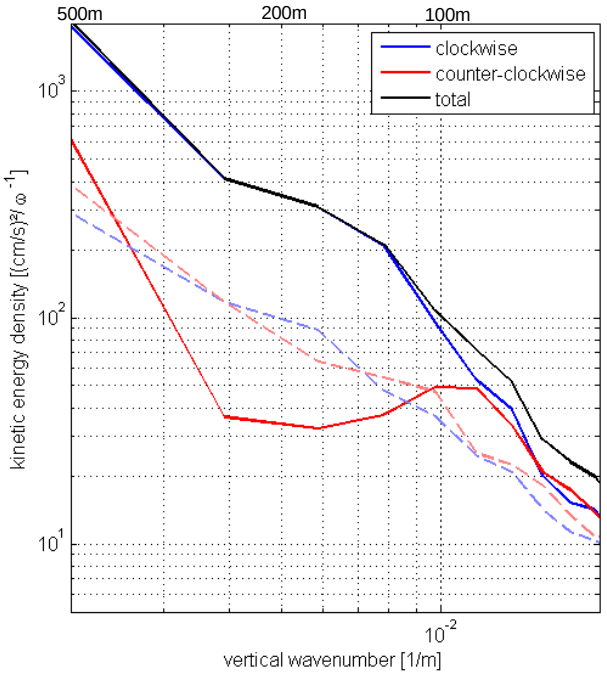

Observed Near Inertial Waves

The slope of lines of the same phase is mainly caused by horizontal gradients in either the density or the vorticity field. As we do not no either of them with sufficient accuracy do remove their effect we turned to small timeseries at times, the ship was standing. Temporal gradients in density or vorticity are neglected. For this time series the slope of the phases in these Hovmöller-diagrams is only caused by the phase velocity.

However, these timeseries are too short to gain robust results for the phase velocity as they only cover a fraction of a wave period.

On the right, lines with a slope resulting from a frequency set equal to the local f are drawn in the Hovmöller diagrams, fitting reasonably well.

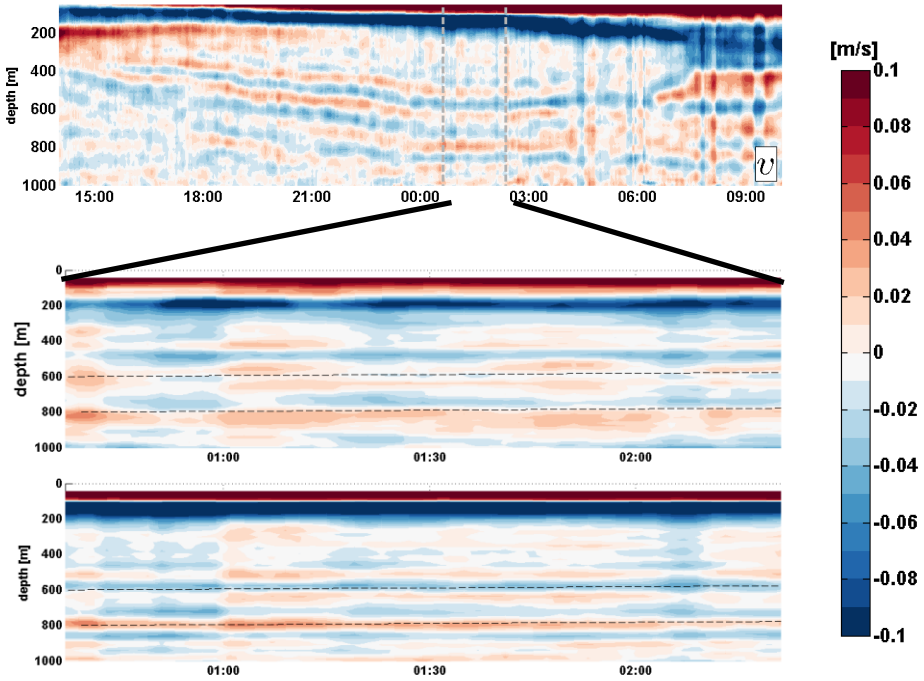

Summary

Using the background density and velocity field the effective Coriolis parameter $f_{eff} = f\sqrt{1 + {}^{\zeta}/_{f}}$

And the 'geostrophic' Richardson number $Ri_g = \frac{(\frac{\partial \bar{u}}{\partial z} + \frac{\partial \bar{v}}{\partial z})^2}{N^2}$ can be calculated.

These are then used to derive $\omega_{min} = f\sqrt{\frac{f_{eff}^2}{f^2} - \frac{1}{Ri_g}}$. (Whitt et al., 2018)

For an internal wave with the frequency $\omega = f$ the vertical group velocity can be calculated as:

$$\omega^2 = f^2 + N^2\frac{K_h^2}{m^2}$$

$$c_{gz} = \frac{\partial \omega}{\partial k} \approx \frac{-N^2K_h^2}{m^3 f}$$

With $f = \omega_{min}$ and $\omega = f$. [Alford et al., 2015]

Note especially, the decreasing downward group velocity below 400m leading to an energy flux convergence!

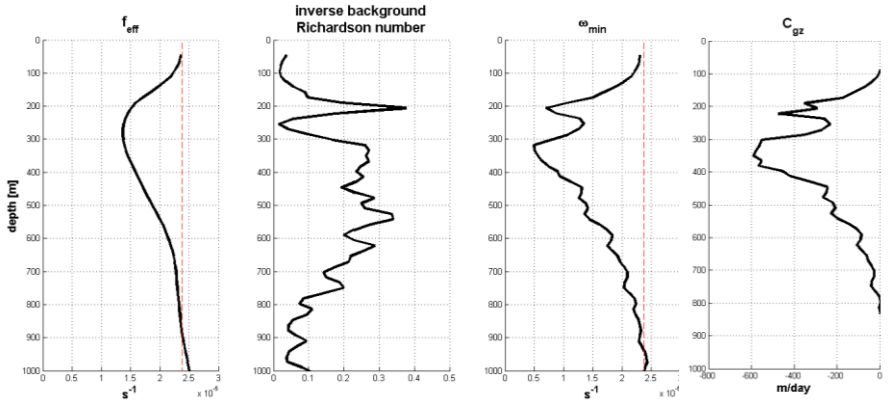

Thank you for your interest!

References:

Mooers, C. N. A technique for the cross spectrum analysis of pairs of complex-valued time series, with emphasis on properties of polarized components and rotational invariants *Deep Sea Research and Oceanographic Abstracts,* **1973**, *20*, 1129-1141

Challenor, P. G.; Cipollini, P. & Cromwell, D. Use of the 3D Radon transform to examine the properties of oceanic Rossby waves *Journal of Atmospheric and Oceanic Technology,* **2001**, *18*, 1558-1566

Whitt, D. B.; Thomas, L. N.; Klymak, J. M.; Lee, C. M. & D'Asaro, E. A. Interaction of superinertial waves with submesoscale cyclonic filaments in the north wall of the Gulf Stream *Journal of Physical Oceanography,* **2018**, *48*, 81-99

Leaman, K. D. & Sanford, T. B. Vertical energy propagation of inertial waves: A vector spectral analysis of velocity profiles *Journal of Geophysical Research, Wiley Online Library,* **1975**, *80*, 1975-1978

Alford, M. H.; MacKinnon, J. A.; Simmons, H. L. & Nash, J. D. Near-inertial internal gravity waves in the ocean *Annual review of marine science, Annual Reviews,* **2016**, *8*, 95-123

Shcherbina, A. Y.; D'Asaro, E. A.; Lee, C. M.; Klymak, J. M.; Molemaker, M. J. & McWilliams, J. C. Statistics of vertical vorticity, divergence, and strain in a developed submesoscale turbulence field *Geophysical Research Letters, Wiley Online Library,* **2013**, *40*, 4706-4711

For any further questions or discussions feel free to contact me:

E-mail: daniel-rudloff@gmx.net